Green Removal of Toxic Pb(II) from Water by a Novel and Recyclable Ag/γ-Fe_2O_3@r-GO Nanocomposite

Haerizade, Bibi Narjes
Young Researchers and Elites Club, Qom Branch, Islamic Azad University, Qom, I.R. IRAN

Ghavami, Monireh
Industrial and Mechanical Engineering Department, Qazvin Branch, Islamic Azad University, P.O. Box 34185-1416 Qazvin, I.R. IRAN

Koohi, Maryam
Young Researchers and Elites Club, North Tehran Branch, Islamic Azad University, Tehran, I.R. IRAN

Janitabar Darzi, Simin
Nuclear Science and Technology Research Institute, 11365-8486, Tehran, I.R. IRAN

Rezaee, Nasibeh; Kassaee, Mohammad Zaman*[+]
Department of Chemistry, Tarbiat Modares University, P.O. Box 14115-175, Tehran, I.R. IRAN

ABSTRACT: *Toxic leadions removed efficiently from water by a newly fabricated, magnetically recyclable, antibacterial nano-Ag/γ-Fe_2O_3@GOadsorbent, at ambient and the physiological pH=7. The adsorption depends on the adsorbent dosage, initial Pb(II)concentration, pH and the contact time. The optimum* removal *efficiency of the leadion is found to be 93.1% with a dosage rate of 20 mg/L, in 40 minutes, at pH 5 (to 14). Equilibrium data fits well with the Langmuir and Freundlich models with a maximum adsorption capacity of 90.91 mg/g of Pb(II) per 20 mg/L of Ag/γ-Fe_2O_3@GO. The removal/uptake mechanism involves interaction between Pb(II) and the oxide/hydroxyl layer around Ag/γ-Fe_2O_3@rGO, in the contaminated water medium.*

KEYWORDS: *Pb(II); Ag/γ-Fe_2O_3@GO; Adsorbent; Adsorption isotherms; Batch; Removal.*

INTRODUCTION

Heavy metals released in the ecosystem often cause serious environmental and health risks. They are commonly toxic even at low concentrations [1-4]. Among them, lead is one of the most distributed and has been regarded as a serious hazardous heavy metal in the context of environmental risk [5, 6].

** To whom correspondence should be addressed.*
+ E-mail: kassaeem@modares.ac.ir
1021-9986/2018/1/29-37 9/$/5.09
DOI:

Nowadays, numerous methods have been proposed for efficient heavy metal removal from water, including but not limited to chemical precipitation, ion exchange, adsorption, membrane filtration and electrochemical technologies [7-10]. Between these techniques, adsorption offers flexibility in design and operation. In many cases, it generates high-quality treated effluent. Also, owing to the reversible nature of most adsorption processes, the adsorbents may be regenerated by suitable desorption processes for multiple uses [11]. In addition, many desorption processes are of low maintenance cost, high efficiency, and ease of operation [12]. So, adsorption is recognized as an effective and economic method for Pb(II) removal from wastewaters. Several various adsorbents have been used for removal of lead [13-20]. Carbon materials have been chosen as an adsorptive media for removal of lead by many researchers [19]. Especially, graphene oxide(GO) based composite materials have been studied as the absorbents [21, 22].

It is known that the carbon materials have excellent biocompatibility with bacteria. So, bacteria might breed on carbon-based adsorbents during the purification process and make these adsorbents themselves pollutants. Moreover, this phenomenon could saturate the adsorbent surface and reduce the efficiency of lead removal. To address this problem, some researchers have explored depositing colloidal-sized silver, a wide-spectrum antibacterial agent, onto the carbon as bactericide [19].

GO is negatively charged due to the distribution of hydroxyl and epoxy groups on its surface as well as the location of carboxyl and carbonyl groups at its edges. They arise from the oxidation of graphite in the presence of strong acid and oxidants. The oxygenated graphene oxide can ensure tremendous opportunities for its functionalized based materials. Therefore, the growing seed or precursor of nanomaterials can be bound onto the GO surface through the electrostatic interactions or chemical modifications. Because of GO are much more applicable than more expensive nanomaterials such as functionalized CNTs, it can be readily obtained from cheap natural graphite in large scale and hybrid multifunctional materials [23]. Graphene oxide has a large number of oxygenated functionalities and high surface area, making it useful for environmental and biological applications. Furthermore, GO-based composite might be attractive in catalytic, photo-catalyst, solar energy conversion fields and heavy metal removal studied [24-31]. Even though GO is a good adsorbent for many ions, its efficient removal from the water after the treatment is still challenging. According to the literature, GO as sorbent of heavy metals has some disadvantages such as low sorption selectivity and difficulty in solid-liquid separation [32]. The 2D-GO nanosheets are strongly hydrophilic and can generate a stable aqueous suspension due to the cover with epoxy, hydroxyl, and carboxyl groups on its panel and edge [24]. On the other side, abundant hydrophilic hydroxyl and carboxyl groups on GO can easily coordinate with metals and metal oxides [33]. Magnetic nanoparticles are useful because of their key properties such as magnetic separation and ease to functionalize with various chemical groups to increase their affinity toward target compounds. In this research, we have synthesized an Ag decorated graphene oxide magnetic nanocomposite, Ag/Fe2O3@GO (Scheme 1), and investigated its use for removal of Pb contamination from water.

EXPERIMENTAL SECTION

Materialandinstruments

Natural flake graphite used to prepare graphene oxide (GO) nanoparticles is fabricated by mixing ferric chloride hexahydrate ($FeCl_3.6H_2O$, Aldrich, 98%), ferrous chloride tetrahydrate ($FeCl_2.4H_2O$, Aldrich, 98%), deionized water (DI water), and ammonium hydroxide (NH_4OH, Merck, 25%). For the preparation of GO from graphite, H_2SO_4 (98%), H_2O_2 (30%) and potassium permanganate ($KMnO_4$) are used. For the preparation of Ag nanoparticle (AgNPs) $AgNO_3$ and $NaBH_4$ are used from Aldrich Co. A stock solution of Pb(II) is prepared (50 mg/L) by dissolving the required amount of $Pb(NO_3)_2$ in double distilled water. The stock solution is diluted with double distilled water to obtain the desired concentration, ranging from 5 to 30 mg/L. All purchased compounds are used as received, with no further purification. FT-IR spectra are recorded using KBr pellets with a thermo-spectrometer. Samples are characterized by XRD diffractometer (Philips X'pertMPD, CoKα irradiation, λ¼1. 78897Å. In addition, TEM (ZEISS, EM10C, at 80 kV of acceleration voltage) is employed to observe the morphology of Ag/Fe_2O_3@r-GO nanocomposites.

Preparation of GO

GO is prepared using Hummers method [34, 35]. Graphite (1 g) is added to 100 mL of concentrated sulfuric acid in an ice bath. Then 4 g of potassium permanganate is gradually added while stirring. The solution is stirred for 2 h at temperatures below 10 °C, followed by 1 h at 35°C until a thick paste is formed. After that, it is diluted with 100 mL of deionized (DI) water in an ice bath and the temperature is raised to 98 °C in a water bath, then it is stirred for 1 h. The mixture is diluted again to 300 mL. Then, 20 mL of hydrogen peroxide (30%) is added. The color changes to a brilliant yellow. The resultant is centrifuged and washed several times with hydrogen chloride (5%), and then by DI water until the pH of the supernatant becomes neutral. As a final point, the resulting solid is dried at 60 °C for 24h, and a loose brown powder is formed.

Preparation of Fe_2O_3@GO

40 mg of GO is added to 40 mL of water and ultrasonicated for 30 min. A 50mL solution of $FeCl_3$ (800mg) and $FeCl_2$ (300mg) in DI water is added to it at ambient. The temperature is gently raised to 85 °C. An ammonia solution (30%) is added until the pH increases to 10. After stirring for 45 min the solution is cooled to room temperature. At last, the resulting black precipitate is centrifuged at 4000 rpm for 15 min, washed three times with DI water and dried at 60 °C [37].

Preparation of Ag/Fe_2O_3@GO

200 mg of Fe_2O_3@GO powder is dispersed in 100 mL of DI water through ultrasonication for 30 min while stirring, 50 mg silver nitrate is added to the resulting stable colloid. The mixture is moved to a 100 °C oil bath while stirring strongly. Then an aqueous solution of $NaBH_4$ (1 mg/mL) is added. After 5 min, the mixture is cooled down to 60 °C and stirred for 2 h. Finally, the resulting crude is washed with ethanol and DI water and dried at 60 °C for 24 h.

Removal of lead

A standard solution of Pb(II) is prepared (50 mg/l) by dissolving the required amount of $Pb(NO_3)_2$ in DI water. It is diluted with DI water to reach the desired concentrations (5, 10, 15, 20, 25 and 30 mg/L). Batch adsorption experiments are carried out by contacting 20 mg of Ag/γ-Fe_2O_3@r-GO with 50 mL of an aqueous solution of the above different primary concentrations (5 to 30 mg/L) at natural pH solution (pH=5) and room temperature. After adsorption reaches a state of equilibrium, the adsorbent is separated *via* an external magnet and then can be readily re-dispersed with slightly shaking. The results reveal that the particles exhibit well magnetic responsible and re-disperse property, suggesting them as a potential application of adsorbents. The concentration of lead is measured by an inductively coupled plasma optical emission spectrometer (ICP-OES). Removal efficiency is calculated using the following relationship (Eq. (1)):

$$\%E = \left[\frac{(C_0 - C_e)}{C_0}\right] \times 100 \quad (1)$$

Here, Ce and $C_0$are the equilibrium and initial concentrations of Pb(II) (mg/L), respectively and *E*, is the removal efficiency.

Adsorption isotherms

20 mg of Ag/Fe_2O_3@GO is added to 50 mL solutions containing Pb(II) concentrations of 5–30 mg/L, at pH=5. Each bottle is rotated at 400 rpm for 30 min. After adsorption reaches the state of equilibrium, the adsorbent is separated *via* an external magnet. Residual concentrations of lead are determined with an Inductively Coupled Plasma Optical Emission Spectrometer (ICP-OES). The specific amount of lead adsorbed is calculated from the following equation:

$$q_e = V\left[\frac{(C_0 - C_e)}{m}\right] \quad (2)$$

Here q_e (mg/g) is the equilibrium adsorption capacity; C_0 and *Ce* (mg/L) are the initial and equilibrium concentrations of the adsorbate in solution, respectively. *V* is the volume (mL) of the lead aqueous solution and *m* is the mass (mg) of adsorbent used in the experiments.

RESULTS AND DISCUSSION

Magnetically recyclable, antibacterial Ag/γ-Fe_2O_3@rGO is synthesized and applied as an adsorbent for removal of toxic lead from water. The structure of the adsorbent is characterized by FT-IR, XRD, and TEM. Effects of different parameters are investigated, including

Scheme 1: Preparation of Ag/γ-Fe_2O_3@r-GO nanocomposite.

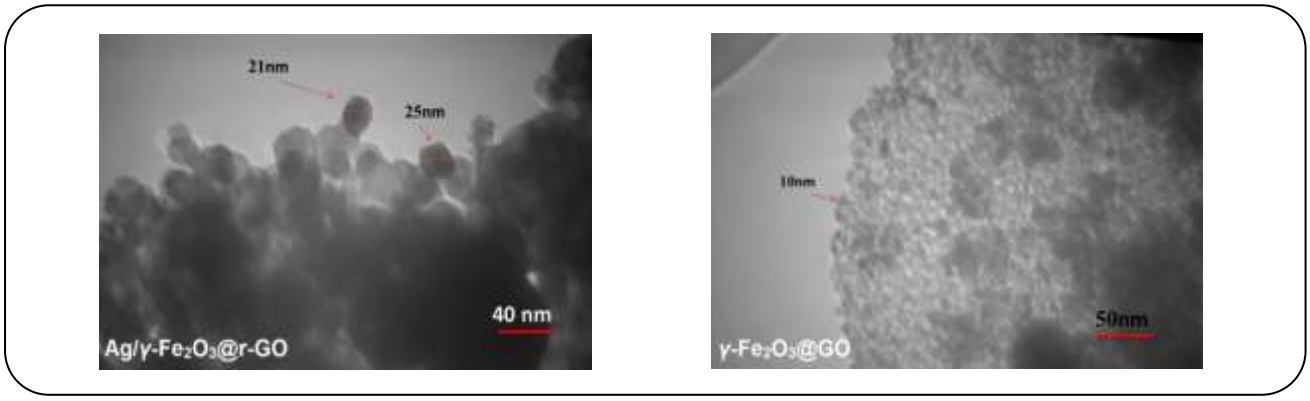

Fig. 1: TEM images of GO, Fe_2O_3@GO and Ag/γ-Fe_2O_3@r-GO nanoparticles.

contact time, adsorbent concentration, pH, and the initial concentration of Pb(II).

Characterization of adsorbent

TEM images of prepared Ag/γ-Fe_2O_3@r-GO nanocomposite involve dark and light parts, which darker areas are for Ag nanoparticles, whereas the lighter areas are for γ-Fe_2O_3 nanoparticles (Fig. 1). Average diameters of darker and lighter nanoparticles are 21-24 and 10nm, respectively.

FT-IR spectra of the GO, Fe_2O_3@GO and Ag/γ-Fe_2O_3@r-GO nanocomposites are compared and contrasted to confirm the coexistence of nanosilver (Fig. 2). The characteristic peaks at 3415, 1717,1619,1343,1183 and 1047cm^{-1} of GO are assigned to the –OH stretching vibrations, C=O stretching of COOH groups, skeletal vibrations of un-oxidized graphitic domains, O–H deformations of the C–OH groups, epoxy symmetrical ring deformation vibrations and C–O stretching vibrations, respectively (Fig. 2a). In contrast, to GO spectrum, Fe_2O_3@GO spectrum shows weaker peaks for C=O, C–O and O–H (1717, 1183, 1047 and 3421 cm^{-1}, respectively, Fig. 2b). Also, typical peak presented at 571 cm^{-1} confirms the Fe–O vibrations. This indicates that GO is coated by Fe_2O_3 successfully. A new absorption band at 1565 cm^{-1} of Ag/γ-Fe_2O_3@r-GO nanocomposite spectrum, shows the skeletal vibration of the graphene sheets (Fig. 2c). This may be determined that GO is reduced to G.

XRD patterns of GO, Fe_2O_3@GO, and Ag/γ-Fe_2O_3@r-GO nanocomposites are compared and contrasted (Fig. 3). The obtained XRD pattern for GO shows a diffraction peak at 10.58ºattributed to the diffraction on its (002) layer planes with the basal spacing of 0.959 nm (Fig. 3a). There is a peak at 22.29º which is interpreted in terms of the short-range order in stacked graphene sheets. For Fe_2O_3@GO nanocomposite, the characteristic peak at2θ=34.97º, 41.53º, 50.41º, 62.81º, 67.29º, and 74.33º related to the (220), (311), (400), (422), (511) and (440) planes of a cubic unit cell of magnetite,

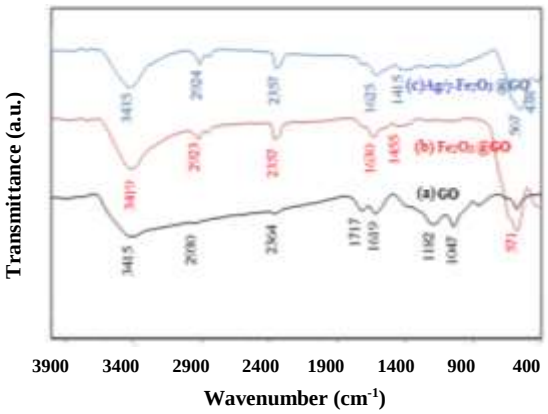

Fig. 2: FT-IR spectra of synthesized GO (a), Fe_2O_3@GO (b), and Ag/Fe_2O_3@GO (c).

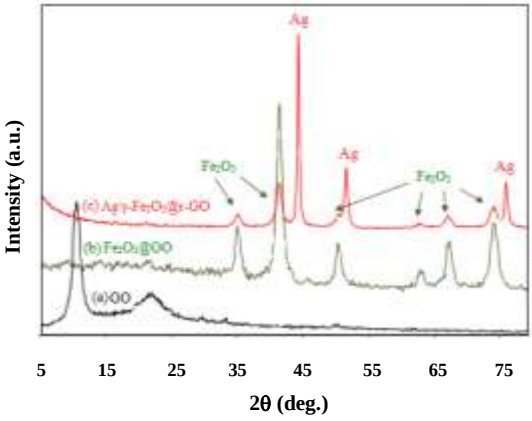

Fig. 3: XRD patterns of synthesized GO (a), Fe_2O_3@GO (b), and Ag/Fe_2O_3@GO (c).

respectively (Fig. 3b). These are indicating that the GO sheets are covered by Fe_2O_3. The peaks at 2θ=44.57, 51.90, and76.49, in the XRD pattern of Ag/γ-Fe_2O_3@r-GO nanocomposite, are corresponding to the (200), (220) and (311) planes of the cubic Ag crystal (JCPDS No.04-0783), respectively (Fig.3c). They confirmed the formation of Ag nanoparticles.

Pb (II) adsorption

Influence of pH

The influence of pH is investigated at the pH ranges of 1–14 while keeping all the other parameters constant. The removal efficiency of Pb(II) ions appears pH dependent with maximum adsorption emerging at pH=5, at room temperature (Fig.4). In a more acidic solution, the protonation of nano Ag and nano Fe_2O_3occurs and there is a weak tendency for the reaction between Pb(II) and Ag/γ-Fe_2O_3@r-GO nanocomposite, which leads to the decrease in the adsorption. On the other hand, at a pH above of 5, rather a negligible drop of adsorption occurs. This is because the Pb(II) ions begin to hydrolyze and then form a very small quantity of $Pb(OH)_2$and $Pb(OH)_3^-$ mixture. Compared with Pb(II) ions, these species are unfavorable for adsorption on nano Fe_2O_3 and negatively charged nano-Ag. Nevertheless, adsorption of Pb can occur efficiently at the physiological pH=7. However, since the maximum adsorption takes place at pH=5, it is selected as the pH of choice for all our adsorption experiments.

Influence of adsorbent dose

Percentage removal of Pb(II) initially increases with an increase in the adsorbent dosage. Using over 20 mg/L of the latter, causes Pb(II) removal reach a plateau where it practically levels off (Fig. 5). This may be due to an overlapping of adsorption sites as a result of over-crowding of adsorbent particles [38]. Removal of Pb(II) increases from 69.4 to 93.1% for adsorbent initial concentrations of 10 and20 mg/L, respectively, at pH=5. So, 20 mg/L of adsorbent is used as the optimum dose for all our adsorption experiments.

Influence of contact time

Pb(II) removal efficiency appears directly proportional to the contact time (Fig. 6). At the first twenty minutes, the efficiency of Pb(II) removal changes abruptly from 0% to 87%. Then it levels off to 93% at contact time=40 min. So, optimum contact time is 40min for adsorption of Pb(II) on Ag/γ-Fe_2O_3@r-GO nanocomposite. The quick adsorption at the initial point is possibly due to the high concentration of adsorbent in solution with higher accessibility to the vacant sites.

Adsorption isotherms

Distribution of the adsorbate species between liquid and adsorbent is defined as adsorption isotherms. They are mathematical models that are based on a set of assumptions which relate to the heterogeneity/ homogeneity of the adsorbent. The type of coverage and the possibility of interaction between the adsorbate species brings about Langmuir and Freundlich [37] types of the isotherm. In this work, these models are applied to fit the adsorption equilibrium data of Pb(II) on Ag/γ-Fe_2O_3@r-GO.

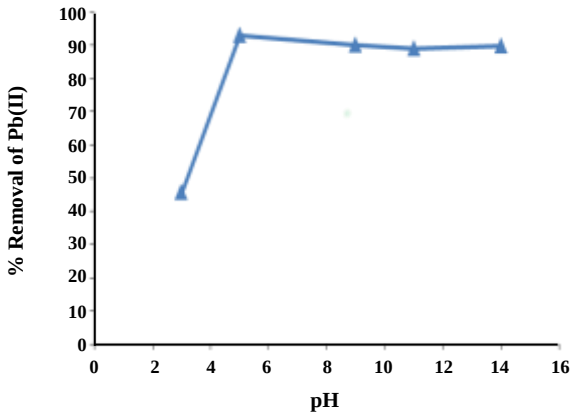

Fig. 4: Adsorption of Pb(II) on Ag/γ-Fe₂O₃@r-GO as a function of pH, using 25 mg/L Pb (II) and 20 mg/L Ag/γ-Fe₂O₃@r-GO.

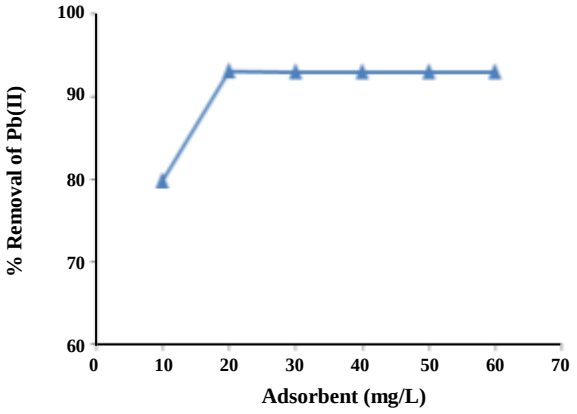

Fig. 5: Adsorption of 25 mg/L Pb(II), over different concentrations of the adsorbent.

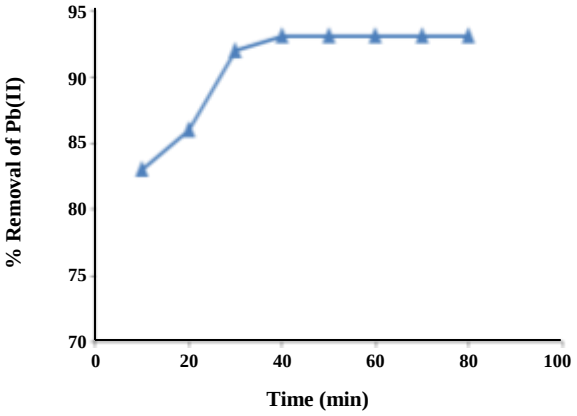

Fig. 6: Adsorption of Pb(II) on Ag/γ-Fe₂O₃@r-GO as a function of contact time using 25 mg/L Pb (II), and 20 mg/L Ag/γ-Fe₂O₃@r-GO, at pH=5.

The Langmuir model describes the statement that maximum adsorption occurs when a saturated monolayer of solute molecules is present on the adsorbent exterior. The linear form of Langmuir equation is as follows:

$$\frac{1}{q_e}=\frac{1}{q_m}+\frac{1}{q_m K_L C_e} \quad (3)$$

Where, C_e(mg/L), q_m (mg/g), and K_L (L/mg) are equilibrium concentration, maximum adsorption capacity, and the Langmuir constant, respectively. Values of K_L and q_m are calculated from the slope and intercept of the linear plot of 1/qe*vs.* $1/C_e$ (Fig. 7). The maximum adsorption capacity obtained for Ag/γ-Fe_2O_3@r-GO is 90.91 mg/g (Table 1).

Furthermore, the dimensionless equilibrium parameter R_L is determined to predict the type of adsorption process, which can be expressed as [38]:

$$R_L=\frac{1}{1+K_L C_0} \quad (4)$$

Where C_0 is the initial Pb(II) concentration (mg/g). The value of R_L shows the type of isotherm. It will be linear for R_L=1, or irreversible for R_L=0. An isotherm is favorable when $0<R_L<1$ or unfavorable when $R_L>1$. To our joy, the R_L value of 0.043specifiesa favorable adsorption between Pb(II) and Ag/γ-Fe_2O_3@r-GO.

The Freundlich isotherm describes equilibrium on heterogeneous surfaces composed of different classes of adsorption sites. The isotherm is shown in Eq. (5) as follows:

$$\log q_e=\log K_F+\frac{1}{n}\log C_e \quad (5)$$

Where, K_F(mg/g) and *n* are the Freundlich parameters related to the adsorption capacity and adsorption intensity, respectively. They can be obtained from the intercept and slop of the plot of log q_e*vs.* log C_e, correspondingly (Fig. 8).

The isotherm data fit the Freundlich model with R^2=0.99 (Tale 1). The Freundlich constants K_f and n are 1.50 mg/g and 0.35 respectively which indicate easy separation of Pb(II) ions from the wastewater. The correlation coefficients show that the adsorption process could be described by both Langmuir and Freundlich models.

Table 1: Langmuir and Freundlich isotherm constants for the adsorption of Pb(II) onto Ag/γ-Fe_2O_3@r-GO.

Langmuir				Freundlich		
q_m (mg/g)	K_L (L/mg)	R_L	R^2	K_F (mg/g)	n	R^2
90.91	0.56	0.043	0.97	1.50	0.35	0.99

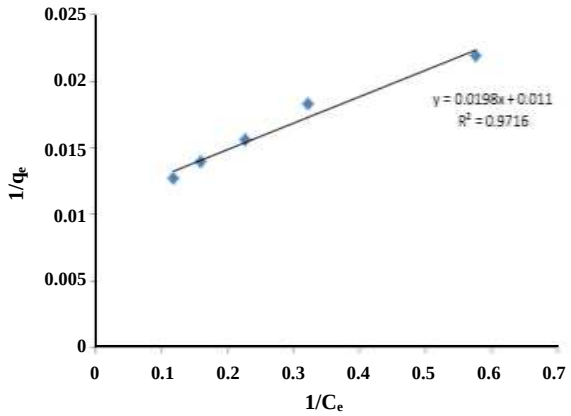

Fig. 7: Langmuir adsorption isotherm for removal of Pb(II) from water via Ag/γ-Fe_2O_3@r-GO.

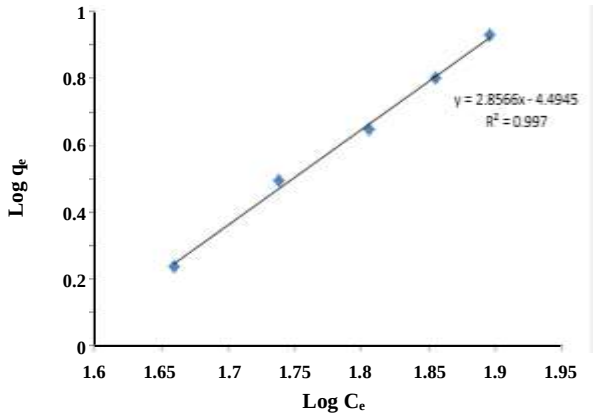

Fig. 8: Freundlich adsorption isotherm for removal of Pb(II) from water via Ag/γ-Fe_2O_3@r-GO nanocomposite.

CONCLUSIONS

For a green removal of lead from water, durable and recyclable Ag/γ-Fe_2O_3@r-GO is prepared. Lead removal increases by increasing the contact time, adsorbent concentration, and pH; while decreases by increasing lead concentration. Optimum(93.1%)removal of lead is achieved *via* Fe nanoparticles (20 mg/L) in 40 min from solution containing 25mg/L of Pb(II), at pH=5. Experimental results are in good agreement with both the Langmuir and Freundlich adsorption isotherm models with a maximum adsorption capacity of 42.9 mg of Pb(II) per 20 mg/L of Ag/Fe_2O_3@GO. Employment of the latter antibacterial magnetic absorbent is foreseen in a near horizon.

Received: Dec. 2, 2016; Accepted: Jul. 10, 2017

REFERENCES

[1] Xu P., Zeng G.M., Huang D.L., Feng C.L., Hu S., Zhao M.H., Lai C., Wei Z., Huang C., Xie G.X. and Liu Z.F., Use of Ion Oxide Nanomaterials in Wastewater Treatment: A Review, *Sci. Total Environ.*, **424**: 1-10 (2012).

[2] Bee A., Talbot D., Abramson S. and Dupuis V., Magnetic Alginate Beads for Pb(II) Ions Removal from Wastewater, *J. Colloid. Interface. Sci.*, **362**: 486-492 (2011).

[3] Bystrzejewski M., Pyrzynska K., Huczko A. and Lange H., Carbon-Encapsulated Magnetic Nanoparticles as Separable and Mobile Sorbents of Heavy Metal Ions from Aqueous Solutions, *Carbon*, **47**: 1201-1204 (2009).

[4] Wang J. and Chen C., Biosorbents for Heavy Metals Removal and Their Future, *Biotechnol. Adv.*, **27**: 195-226 (2009).

[5] Acharya J., Sahu J.N., Mohanty C.R. and Meikap B.C., Removal of Lead(II) from Wastewater by Activated Carbon Developed from Tamarind Wood by Zinc Chloride Activation, *Chem. Eng. J.*, **149**: 249-262 (2009).

[6] Schiewer S., and Balaria A., Biosorption of Pb^{2+} by Original and Protonated Citrus Peels: Equilibrium, Kinetics, and Mechanism, *Chem. Eng. J.*, **146**: 211–219 (2009).

[7] Ghanbari Pakdehi S., Adsorptive Removal of Al, Zn, Fe, Cr and Pb from Hydrogen Peroxide Solution by IR-120 Cation Exchange Resin, *Iran. J. Chem. Chem. Eng. (IJCCE)*, **35**: 75-84 (2016).

[8] Zeng G.M., Li X., Huang J.H., Zhang C., Zhou C.F., Niu J., Shi L.J., He S.B., Li F., Micellar-Enhanced Ultrafiltration of Cadmium and Methylene Blue in Synthetic Wastewater Using SDS, *J. Hazard. Mater.*, **185**: 1304–1310 (2011).

[9] Guo H.J., Luo S.L., Chen L., Xiao X., Xi Q.A., Wei W.Z., Zeng G.M., Liu C.B., Wan Y., Chen J.L. He Y.J., Bioremediation of Heavy Metals by Growing Hyperaccumulaorendophytic Bacterium Bacillussp L14, *Bioresour. Technol.*, **101**: 8599–8605 (2010).

[10] Li X., Zeng G.M., Huang J.H., Zhang D.M., Shi L.J., He S.B., Ruan M., Simultaneous Removal of Cadmium Ions and Phenol with MEUF Using SDS and Mixed Surfactants, *Desalination*, **276**: 136–141 (2011).

[11] Pan B.J., Pan B.C., Zhang W.M., Lv L., Zhang Q.X., Zheng S.R., Development of Polymeric and Polymer-Based Hybrid Adsorbents for Pollutants Removal from Waters, *Chem. Eng. J.*, **151**: 19-29 (2009).

[12] Hua M., Zhang Sh., Pan B., Zhang W., Lv L., Heavy Metal Removal from Water/Wastewater by Nanosized Metal Oxides: A Review, *J. Hazard. Mater.*, **211-212**: 317-331 (2012).

[13] Najiah S., Yusoff M., Kamari A., Putra1 W.P., Ishak C.F., Mohamed A., Hashim N., Md Isa I., Removal of Cu(II), Pb(II) and Zn(II) Ions from Aqueous Solutions Using Selected Agricultural Wastes: Adsorption and Characterisation Studies, *JEP.*, **5**: 289-300 (2014).

[14] Mitra T., Singha B.,Bar N., and Das S.K., Removal of Pb(II) Ions from Aqueous Solution Using Water Hyacinth Root by Fixed-Bed Column and ANN Modeling, *J. Hazard.Mater.*, **273**: 94-103 (2014).

[15] Ma X.J., Li Y.F., Li X.L., Yang L.Q., Wang X.Y., Preparation of Novel Polysulfone Cap-Sules Containing Zirconium Phosphate and their Properties for Pb($^{2+}$) Removal from Aqueous Solution, *J. Hazard. Mater.*, **188**: 296–303 (2011).

[16] Al-Zboon K., Al-Harahsheh M.S., Hani F.B., Fly Ash-Based Geopolymer for Pb Removal from Aqueous Solution, *J. Hazard. Mater.*, **188**: 414-421 (2011).

[17] Hu J., Zhao D.L., Wang X.K., Removal of Pb(II) and Cu(II) from Aqueous Solution Using Multiwalled Carbon Nanotubes/Iron Oxide Magnetic composites, *Water. Sci. Technol.*, **63**: 917-923 (2011).

[18] Tan Y., Chen M., Hao Y., High Efficient Removal of Pb (II) by Amino-Functionalized Fe_3O_4 Magnetic Nano-Particles, *Chem. Eng. J.*, **191**: 104-111 (2012).

[19] Kumar P.S., Vincent C., Kirthika K., Kumar K.S., Kinetics and Equilibrium Studies of Pb^{2+}Ion Removal from Aqueous Solutions by Use of Nano-Silversol-Coated Activated Carbon, *Braz. J. Chem. Eng.*, **2**: 339-346 (2010).

[20] Compton O.C., Nguyen S.T., Graphene Oxide, Highly Reduced Graphene Oxide, and Graphene: Versatile Building Blocks for Carbon-Based Materials, *Small*, **6**: 711-723 (2010).

[21] Seredych M., Bandosz T.J., Adsorption of Ammonia on Graphite Oxide/Aluminiumpolycation and Graphite Oxide/Zirconium-aluminiumpolyoxycation Composites, *J. Colloid. Interface. Sci.*, **324**: 25-35 (2008).

[22] Hummers W.S., Offeman R.E., Preparation of Graphitic Oxide, *J. A. Chem. Soc.*, **80**: 1339-1339 (1958).

[23] Sun H.M., Cao L.Y., Lu L.H., Magnetite/Reduced Grapheme Oxide Nanocomposites: One Step Solvothermal Synthesis and Use as a Novel Platform for Removal of Dye Pollutants, *Nano Res.*, **4**: 550-562 (2011).

[24] Han C., Zhang N., Xu Y.-J., Structural Diversity of Graphene Materials and Their Multifarious Rolesin Heterogeneous Photocatalysis, *Nano Today*, **11**: 351-372 (2016).

[25] Zhang N., Zhang Y., Xu Y.-J., Recent Progress on Graphene-Based Photocatalysts: Current Status and Futureperspectives, *Nanoscale*, **4**: 5792-5813 (2012).

[26] Yang M.-Q., Han C., Zhang N., Xu Y.-J., Precursor Chemistry Matters in Boosting Photoredox Activity of Graphene/Semiconductor Composites, *Nanoscale*, **7**: 18062-18070 (2015).

[27] Zhang N., Xu Y.-J., The Endeavour to Advance Graphene-Semiconductor Composite-Based Photocatalysis, *Cryst. Eng. Comm.*, **18**: 24-37 (2016).

[28] Zhang N., Yang M.-Q., Liu S., Sun. Y., and Xu Y.-J.,Waltzing with the Versatile Platform of Graphene to SynthesizeComposite Photocatalysts, *Chem. Rev.*, **115**: 10307-10377 (2015).

[29] ZhangY., TangZ.R., FuX., and Xu Y.-J.,TiO_2_Graphene Nanocomposites forGas-Phase Photocatalytic Degradation of Volatile Aromatic Pollutant: IsTiO_2_Graphene Truly Different from Other TiO_2_Carbon CompositeMaterials, *ACS Nano*, **4**: 7303-7314 (2010).

[30] Zhang Y.H., Tang Z.R., Fu X.Z., Xu Y.-J., Eneineering the Uniqe 2D mt of Grapheme-TiO_2 Nanocomposite for Photocatalytic Selective Transformation: What Advantage Does Graphene have Over Its Forebear Carbon Nanotube?, *ACS Nano.*, **5**: 7426-7435 (2011).

[31] Seredych M., Tamashausky A.V., Bandosz T.J., Surface Features of Exfoliated Graphite/Bentonite Composites and Their Importance for Ammonia Adsorption, *Carbon*., **46**: 1241-1252 (2008).

[32] Shunli W., Feng H.,Jiayu W.,Wubo W.,Yawei G., Bin G., Rapid and Highly Selective Removal of Lead from Water Using Graphene Oxide-Hydrated Manganese Oxide Nanocomposites, *J. Hazard. Mater.*, **314**: 32–40 (2016).

[33] Dreyer D.R., Park S., Bielawski C.W., Ruoff R.S., The Chemistry of Graphene Oxide, *Chem. Soc. Rev.*, **39**: 228−240 (2010).

[34] Ghavami M., Mohammadi R., Koohi M., Kassaee M.Z., Visible Light Photocatalytic Activity of Reduced Grapheneoxide Synergistically Enhanced by Successive Inclusion of γ-Fe_2O_3, TiO_2, and Ag Nanoparticles, *Mater. Sci. Semico. Proc.*, **26**: 69-78 (2014).

[35] Namasivayam C., Prabha D., Kumutha M., Removal of Direct Red and Acid Brilliant Blue by Adsorption on to Banana Pith., *Bioresour Technol.*, **64**: 77–79 (1998).

[36] Langmuir I., The Adsorption of Gases on Plane Surfaces of Glass, Mica and Platinum, *J. Am. Chem. Soc.*, **40**: 1361–1403 (1918).

[37] Chen A.H., Yang C.Y., Chen C.Y., Chen C.Y., Chen C.W., The Chemically Crosslinked Metal-Complexedchitosans for Comparative Adsorptions of Cu(II), Zn(II), Ni(II) and Pb(II) Ions in Aqueous Medium, *J. Hazard. Mater.*, **163**: 1068-1075 (2009).

[38] Rao G.P., Lu C., Su F., Sorption of Divalent Metal Ions from Aqueous Solution by Carbon Nanotubes: A Review, *Sep. Purif. Technol.*, **58**: 224–231 (2007).